DOI: 10.24850/j-tyca-2026-06-03

Articles

Experimental study of parallel skimming walls effect on sediment reduction in side intakes with sensitivity analysis of geometric parameters

Estudio experimental del efecto de las paredes de desnatado paralelas en la reducción de sedimentos en tomas laterales con análisis de sensibilidad de los parámetros geométricos

Bahador Fatehi-Nobarian[1], ORCID: https://orcid.org/0000-0003-3535-9710

Sadegh Farshidnia[2], ORCID: https://orcid.org/0009-0008-5221-6520

[1]Islamic Azad University, Arak Campus-Department of Civil Engineering, Jolfa, Iran, bfatehinobarian@iau.ac.ir

[2]Islamic Azad University, Tehran Central Branch-Faculty of Engineering-Department of Civil Engineering, Tehran, Iran, farshidnia.sadegh@yahoo.com

Corresponding author: Bahador Fatehi-Nobarian, bfatehinobarian@iau.ac.ir

2026, Instituto Mexicano de Tecnología del Agua. Open Access bajo la licencia CC BY-NC-SA 4.0 (https://creativecommons.org/licenses/by-nc-sa/4.0/)

Tecnología y Ciencias del Agua

OPEN ACCESS

Check for updates

Abstract

Sediment accumulation in channels leads to a variety of challenges that has numerous impacts, ranging from water quality and ecosystem health to infrastructure and flood management. In the present study the main objective was to scrutinize the use of parallel skimming walls to reduce the volume of sediment entering side intakes. The effects of the angle of the skimming walls, wall length, wall height, and the distance between the walls, as well as changes in the main canal flow rate, on the control of sediment entering the intake were studied experimentally. By incorporating hydraulic and geometric variables affecting sediment control, equations for the volume of diverted sediment were derived. The resulting equations were subjected to sensitivity analysis. According to the governing equation of the intake and sediment control, as well as the sensitivity analysis, it was found that the Froude number and the intake flow ratio had the greatest impact on controlling the sediment entering the intake. Furthermore, in all three scenarios examined, the amount of sediment entering the intake with the presence of skimming walls decreased by 58, 70, and 86 %, respectively.

Keywords: Hydraulic structures, hydraulic engineering, canals, hydrodynamics, fluid mechanics, equations, statistical analysis.

Resumen

La acumulación de sedimentos en los canales genera una variedad de problemas con numerosos impactos, que van desde la calidad del agua y la salud de los ecosistemas hasta la infraestructura y la gestión de inundaciones. En el presente estudio, el objetivo principal fue analizar el uso de muros paralelos de desnatado para reducir el volumen de

2026, Instituto Mexicano de Tecnología del Agua.
Open Access bajo la licencia CC BY-NC-SA 4.0
(https://creativecommons.org/licenses/by-nc-sa/4.0/)

sedimento que ingresa a las tomas laterales. Se investigaron experimentalmente los efectos del ángulo de los muros de desnatado, la longitud de los muros, la altura de los muros, la distancia entre ellos, así como las variaciones en el caudal del canal principal sobre el control del sedimento que entra en la toma. Mediante la incorporación de variables hidráulicas y geométricas que afectan el control de sedimentos, se derivaron ecuaciones para el volumen de sedimento derivado. Las ecuaciones resultantes se sometieron a un análisis de sensibilidad. De acuerdo con la ecuación que rige la toma y el control de sedimentos, así como con el análisis de sensibilidad, se encontró que el número de Froude y la relación de caudal de entrada tenían el mayor impacto en el control del sedimento que ingresa a la toma. Además, en los tres escenarios examinados, la cantidad de sedimento que entraba a la toma con la presencia de los muros de desnatado disminuyó en un 58, 70 y 86 %, respectivamente.

Palabras clave: estructura hidráulica, ingeniería hidráulica, canal, hidrodinámica, mecánica de fluidos, ecuación, análisis estadístico.

Received: 30/06/2025

Accepted: 28/02/2026

Available ahead of print: 12/05/2026

Version of record: 01/11/2026

2026, Instituto Mexicano de Tecnología del Agua. Open Access bajo la licencia CC BY-NC-SA 4.0 (https://creativecommons.org/licenses/by-nc-sa/4.0/)

Introduction

As shown in Figure 1. The flow in a water intake branch is generally in three-dimensional form and exhibits several complexities, which can be summarized as follows:

1. Flow separation and vortex formation at the upstream entrance of intake can be observed, leading to secondary currents and sediment deposition.
2. Deflection of the bottom-line flow toward the opposite bank of the intake.
3. Lack of control over incoming sediments.
4. Reduction in sediment transport capacity, resulting in sediment deposition.

2026, Instituto Mexicano de Tecnología del Agua.
Open Access bajo la licencia CC BY-NC-SA 4.0
(https://creativecommons.org/licenses/by-nc-sa/4.0/)

Tecnología y Ciencias del Agua
OPEN ACCESS
Check for updates

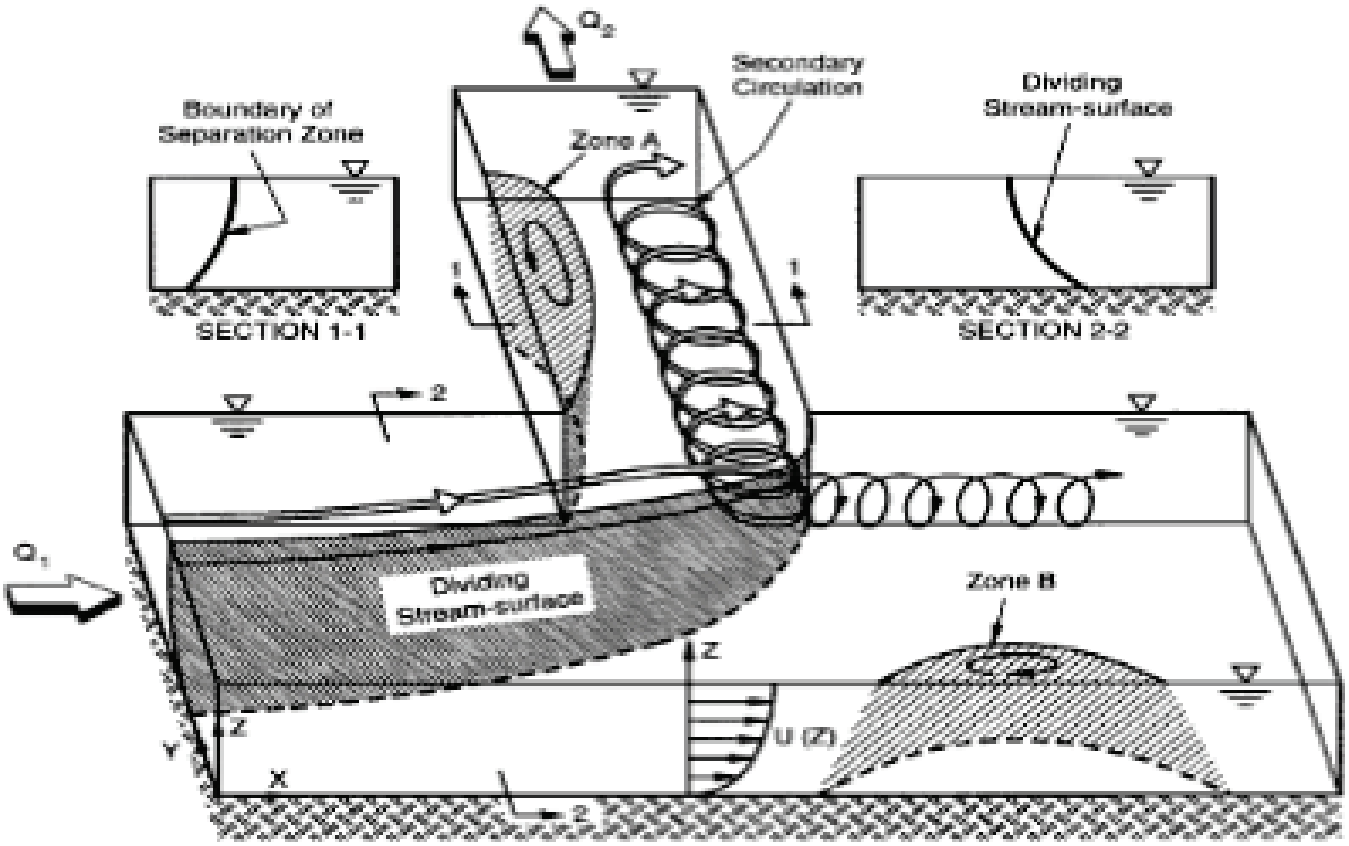


Figure 1. Flow pattern at the side intake location.

The skimming wall itself might be a physical structure, such as a vertical or inclined wall, or even a series of small dams or baffles placed strategically along the drain. These structures reduce the flow velocity and allow the water to move in a more controlled manner. One of the solutions for reducing the volume of sediment entering side intakes is the use of parallel skimming walls in the main canal, located near the intake mouth. The panel that is parallel to the main flow direction can change its angle. These walls create a vortex in the downstream flow, generating shear stress on the riverbed (Barkdoll *et al*., 1999). However, despite the significant role of vortex formation in altering flow dynamics and riverbed

2026, Instituto Mexicano de Tecnología del Agua.
Open Access bajo la licencia CC BY-NC-SA 4.0
(https://creativecommons.org/licenses/by-nc-sa/4.0/)

structure, previous studies have not adequately addressed the associated issue of sediment reduction in channels. While the formation of vortices has been linked to changes in riverbed morphology, limited research has been conducted on how these changes affect sediment transport and deposition, particularly in the context of side intakes. This gap in the literature highlights the need for further investigation into how such vortex-induced flow alterations can be harnessed for effective sediment control and intake optimization. Accordingly, by creating a relatively deep channel along the main canal, sediment can be transferred downstream, which leads to a mitigation in the amount of sediment entering the side intake.

Several studies have explored the impact of skimming walls and other sediment control structures on reducing sediment entry into intakes. Sensitivity analyses have examined parameters such as wall angle, position, intake angle, and the combination of skimming walls with other structures like dikes and weirs. Moradinejad *et al*. (2017) experimentally investigated how the dike's angle and distance from the intake mouth, combined with the skimming wall, affect sediment control and intake efficiency. Results showed that using both skimming walls and dikes effectively reduced sediment entry and improved intake performance (Moradinejad *et al*., 2016). The study involved field surveys, data analysis, and sediment transport modeling using MIKE 21's Sand Transport Module.

Despite findings from sediment transport modeling, the effectiveness of structures like flow divider walls or skimming walls in reducing sediment entry at side intakes remains inadequately addressed in the context of improving intake system efficiency (Wibowo *et al.*, 2020). Consequently, controlling sediment within the channel, particularly at the

2026, Instituto Mexicano de Tecnología del Agua.
Open Access bajo la licencia CC BY-NC-SA 4.0
(https://creativecommons.org/licenses/by-nc-sa/4.0/)

intake, is still a significant challenge in hydraulic engineering requiring further investigation into the direct impact of flow-altering structures on sediment reduction in these critical areas. Submerged vanes, hydrofoils used to manage river sediment transport by generating helical turbulence, are placed at specific angles to the flow. One study aimed to analyze the effect of rows of these vanes on flow turbulence characteristics such as intensities, Reynolds stresses, turbulent kinetic energy, anisotropy index, and velocity profiles (Sharma & Ahmad, 2020). The study considered two softscape elements: the visible water area and the vegetation. These were quantified as the percentage of visible water (WR) and the percentage of visible greenery (GR). The findings indicated that people's visual preferences were significantly influenced by how harmonious these elements appeared. Specifically, participants preferred a composition of 30 % visible water and 40% visible greenery to achieve the best harmony, naturalness, and overall visual appeal of the sediment control structures (Chen *et al*., 2020). Sediments discharge and Shields number were measured and computed for the given hydraulic conditions. Afterwards, it was concluded that Meyer-Peter and Müller equation can also be applied for other hydraulic conditions and similar procedure may be adopted in order to calibrate the dimensionless Meyer-Peter and Müller number at other cases (Kuriqi *et al*., 2020).

Nakato and Odgen (1998) used submerged plates for sediment control at the intake of the Kansai Bluffs power plant. They stated that after 3.5 years of installation, there was no need for dredging, and the intake did not encounter any sediment-related issues. Barkdoll *et al*. (1999) investigated ways to increase the efficiency of submerged plates. After experimental testing of various strategies to increase intake efficiency while maintaining the performance of the submerged plates,

2026, Instituto Mexicano de Tecnología del Agua.
Open Access bajo la licencia CC BY-NC-SA 4.0
(https://creativecommons.org/licenses/by-nc-sa/4.0/)

the use of skimming walls alongside submerged plates and widening the intake mouth were identified as effective solutions. Johnson *et al*. (2001) recommended an angle of 25-30° for submerged plates to generate maximum secondary flow and, as a result, to reduce sediment entry into the intake. Hsu *et al*. (2002) studied the intake canal, which is aligned with the main canal, showing that as the ratio of diverted flow was increased, the ratio of upstream flow depth to downstream flow depth in the main canal also increased, and this ratio was further increased with a decrease in the Froude number. Davoodi and Shafai-Bajestan (2012) examined sediment control using submerged plates in front of side intakes in trapezoidal channels.

Their experiments were conducted at four different distances (4, 6, 8, 10 times the water depth) for four Froude numbers of 0.45, 0.55, 0.60, and 0.66. In all experiments, the intake ratio was kept constant at 7.5 %. Halvaeifard and Masjedi (2017) studied the effect of the angle 25° of submerged plates on the relative diverted flow in curved channels with the presence of submerged plates. Tabrizi *et al*. (2017) investigated the impact of dike structures on modifying the flow pattern of diverted water into intakes located in bends. The results of this study showed that the sediment diversion ratio was affected by the intake ratio and had a direct relation with its increase. Moradinejad *et al*. (2017) experimentally studied sediment control using skimming walls and dikes at the mouth of side intakes.

The results showed that, with the presence of skimming walls combined with dikes, the amount of sediment entering the intake decreased by 81 % with a skimming wall at angle 10°, 78 % with a skimming wall at angle 14°, and 76 % with a skimming wall at angle 18°.

2026, Instituto Mexicano de Tecnología del Agua.
Open Access bajo la licencia CC BY-NC-SA 4.0
(https://creativecommons.org/licenses/by-nc-sa/4.0/)

Attarzadeh and Ghodsian (2018) experimentally examined the efficiency of various systems combining different sizes of sill, dike, and submerged plates for controlling sediment entry into side intakes with angle 90° at intake ratios of 0.12, 0.15, and 0.18. The results indicated that the dike and submerged plates had a significant impact on sediment control, and in some cases, achieved nearly 100 % efficiency in eliminating sediment entry into the intake. Golej *et al*. (2019) performed experiments in a U-shaped channel to test methods for controlling sediment entering intakes. Their key finding was that using a combination of a sill, a dike, and a skimming wall was most effective at preventing sediment from entering the intake, achieving a 92 % reduction in incoming sediment compared to scenarios where no control structures were used.

Bor (2022) investigated two experiments that were performed in a 90° water intake to study 3D flow patterns and sediment distribution using submerged vanes under sediment feeding and live-bed conditions. Three vanes were installed at a 20° angle, maintaining a water discharge ratio of qr≈<5>0.1. Three-dimensional mean and turbulent velocity components of flow in a 90° channel intake were measured using acoustic Doppler velocimetry (ADV). Results showed that three vanes with a single column reduced sediment by 20 % during diversion. High velocities and scour were observed at the downstream corner of the intake.

Existing studies do not adequately explore how these parallel walls can be optimized for further sediment reduction in intake systems, creating a gap in the research. However, further research is needed to explore the behavior of flow and sediment around submerged vanes, as well as the potential of flow divider walls for better sediment control (Mandal *et al*., 2024).

2026, Instituto Mexicano de Tecnología del Agua.
Open Access bajo la licencia CC BY-NC-SA 4.0
(https://creativecommons.org/licenses/by-nc-sa/4.0/)

Habibi *et al*. (2019) studied the effect of submerged plates on sediment-laden flow in river bends, highlighting the importance of plate geometry in controlling sediment entry into side intakes. The results of this study showed that as the intake ratio was increased, the length and relative width of the vortex region were decreased. The efficiency of the plates in preventing sediment entry into the side intake and guiding surface flow toward the intake mouth was maintained.

In this study, a clear research gap is evident, as previous studies have not specifically addressed the impact of flow divider walls on reducing sediment entry into side intake systems in channels. Although there exist numerous studies with a focus on using structures such as submerged plates, dikes, and other methods for sediment control at intakes, none of these studies have thoroughly examined the effect of flow divider walls in a laboratory setting with high precision.

Based on the research background, most studies conducted on sediment control entering intakes have focused on submerged plates, sills, dikes, or their combinations. Therefore, further studies are required, particularly in cases where parallel skimming walls are used in front of the intake.

To demonstrate the effects of the angle of the parallel skimming walls (θ), the distance between the two skimming walls (b), the length of the skimming walls (L), and the height of the skimming walls (H) on the amount of sediment entering the intake, two parallel skimming walls should be used, and equations between these parameters and the volume of sediment entering the intake under different conditions should be derived. The main objective of this study is to investigate and analyze the effect of parallel skimming walls in controlling sediment entering side intakes from rectangular channels. By using these walls, the study aims

2026, Instituto Mexicano de Tecnología del Agua. Open Access bajo la licencia CC BY-NC-SA 4.0 (https://creativecommons.org/licenses/by-nc-sa/4.0/)

to explore the distribution and movement of sediments entering the system.

This research intends to derive complex equations relating various parameters such as flow velocity, wall angle, and sediment characteristics, ultimately providing an analytical model for optimal intake design, which is one of its innovations. Additionally, sensitivity analysis has been conducted thoroughly to evaluate the accuracy and performance of the models and examine the impact of parameter variations on the obtained results. This study not only focuses on the practical aspects of intake design but contributes to a better understanding of sediment behavior in similar hydraulic systems.

In general, another innovation and main aim of this research is the introduction of a practical model for reducing sediment in inlet channels leading to reservoir dams. Moreover, such a precise system can be applied to side weirs of dams to enhance the performance of rectangular side weirs. This approach has not been previously studied with such a scientific perspective, and it can be considered a research gap that remains unaddressed. The use of flow skimming walls for controlling sediment entry into side intakes can be traced back to past studies on submerged plates. Key design parameters of submerged plates include plate height, length, flow impact angle, both longitudinal and transverse spacing. In addition to protecting riverbanks, flow skimming walls play a crucial role in diverting bed-load sediments away from intake entrances and controlling sediment deposition. These structures generate a downstream rotational flow that induces transverse shear stress on the riverbed. The vortices formed at the lower edge of the wall are carried downstream, where they merge into larger vortices. This vortex system creates a helical motion, which alters the bed shear stress along the main channel

2026, Instituto Mexicano de Tecnología del Agua.
Open Access bajo la licencia CC BY-NC-SA 4.0
(https://creativecommons.org/licenses/by-nc-sa/4.0/)

near the intake entrance, thus effectively transporting sediments downstream.

Figure 2 shows a schematic of research.

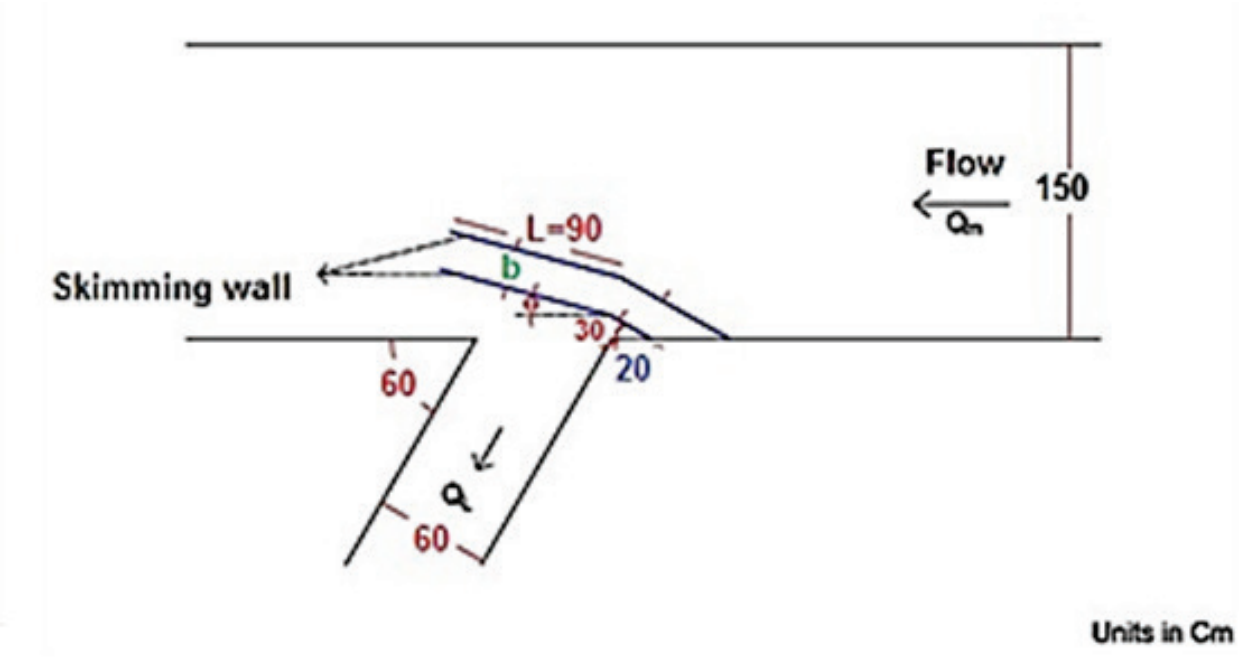


Figure 2. Experimental flume plan and the placement of parallel skimming walls.

Method and materials

The governing equations for skimming walls in controlling sediment in side intakes are based on fluid dynamics, sediment transport, and flow separation principles. The key equations come from the Navier-Stokes equations, the continuity equation, and sediment transport equations. The followings are the fundamental equations governing the process:

2026, Instituto Mexicano de Tecnología del Agua.
Open Access bajo la licencia CC BY-NC-SA 4.0
(https://creativecommons.org/licenses/by-nc-sa/4.0/)

Continuity equation (Mass Conservation). For an incompressible fluid, the continuity equation ensures that the flow rate remains consistent:

$$\frac{\partial u}{\partial x} + \frac{\partial v}{\partial y} + \frac{\partial w}{\partial z} = 0 \quad (1)$$

Where:

u,v,w, = velocity components in the x,y,z directions, respectively.

In the presence of a skimming wall, part of the flow is redirected, creating a separation zone that influences sediment deposition**.** The sediment transport equation, sediment transport is typically modeled using the Exner equation (for bed load transport), so-called the advection-diffusion equation (for suspended load transport):

$$\frac{\partial C}{\partial t} + \nabla \cdot (CU) = \nabla \cdot (D\nabla C) + S \quad (2)$$

Where:

∇ = Nabla Operation

$\nabla \cdot (CU)$ = this term involves the gradient of the product of sediment concentration (C) and the velocity vector (U)

$\nabla \cdot (D\nabla C)$ = this term involves the gradient of the sediment concentration gradient (∇C), multiplied by the diffusion coefficient (D)

C = the sediment concentration, which indicates the amount of sediment present in the water column at a given location

2026, Instituto Mexicano de Tecnología del Agua.
Open Access bajo la licencia CC BY-NC-SA 4.0
(https://creativecommons.org/licenses/by-nc-sa/4.0/)

U = velocity vector, describing the flow velocity of the water in which sediment is suspended, affecting its transport and distribution

D = diffusion coefficient, representing the rate at which sediment spreads due to molecular diffusion or turbulent mixing in the water

S = the sediment source/sink term, accounting for any external factors that add or remove sediment from the system, such as sediment deposition, erosion, or external inputs

At the skimming wall, flow separation occurs, reducing turbulence in the lower layers and encouraging sediment deposition before reaching the side intake. The Shields parameter for sediment motion was used to determine if sediment will settle or remain suspended, the Shields parameter (θ) is defined as below:

$$\theta = \frac{\tau_b}{(\rho_s - \rho)gd} \quad (3)$$

Where:

τ_b = bed shear stress.

ρ_s = sediment density.

g = gravitational acceleration.

d = sediment grain diameter.

If θ is below the critical threshold (θc), sediment will settle, which is the goal of skimming walls.

Given that there are many parameters affecting the entry of bed-load sediment into the intake mouth, dimensionless numbers were used to analyze the influence of these parameters. For this purpose, a series

2026, Instituto Mexicano de Tecnología del Agua.
Open Access bajo la licencia CC BY-NC-SA 4.0
(https://creativecommons.org/licenses/by-nc-sa/4.0/)

of dimensionless groups were formed using the Buckingham's dimensional analysis method (see supplemental data 1).

Considering that some parameters were constant, as specified in Table 1, dimensional analysis was used to identify the effective parameters in the studied phenomenon, and the corresponding dimensionless ratios were determined. The final dimensionless equation can be expressed as follows:

$$f\left(\frac{Q_L}{Q_m}; F_r; \frac{V}{D^3}; \frac{b}{H}; \frac{L}{b}; \theta\right) = 0 \quad (4)$$

The ratio of the intake channel flow to the main channel flow:

$Q_R = \frac{Q_L}{Q_m}$ = Froude number (Fr) of the upstream flow at the intake.

$C_s = \frac{V}{D^3}$ = volume of sediment entering the intake to the flow depth cubed (sediment diversion volume ratio).

$\frac{b}{H}$ = distance between the two skimming walls to the height above the bed of the skimming wall.

$\frac{L}{b}$ = length of the skimming wall to the distance between the two skimming walls.

θ = angle of the second branch of the skimming wall with the horizontal axis.

2026, Instituto Mexicano de Tecnología del Agua.
Open Access bajo la licencia CC BY-NC-SA 4.0
(https://creativecommons.org/licenses/by-nc-sa/4.0/)

Table 1. The data used in Equation (9).

Rows	b (m)	Q_R	F_r	b/H	L/b	$C_{s1}(Obs)$	$C_{s2}(Cal)$
1	0.1	0.16	0.30	2.5	9	0.96	0.94
2	0.1	0.28	0.37	2.5	9	1.13	1.15
3	0.1	0.35	0.45	2.5	9	1.56	1.59
4	0.1	0.43	0.56	2.5	9	2.28	2.32
5	0.2	0.16	0.30	5	4.5	0.69	0.61
6	0.2	0.28	0.37	5	4.5	0.82	0.75
7	0.2	0.35	0.45	5	4.5	1.10	1.03
8	0.2	0.43	0.56	5	4.5	1.64	1.51
9	0.3	0.16	0.30	7.5	3	0.32	0.47
10	0.3	0.28	0.37	7.5	3	0.54	0.58
11	0.3	0.35	0.45	7.5	3	0.74	0.80
12	0.3	0.43	0.56	7.5	3	1.09	1.17

Technical specifications and dimensions of the flume used in the experiments

The experiments were conducted at the Soil and Water Conservation Research Institute in Tehran, in a flume with a length of 12 m, width of 1.5 m, and height of 0.9 m, equipped with a water circulation system. The intake was made through a side channel with a width of 0.6 m, length of 2.5 m, and an angle relative to the flow direction in the main channel. The main channel had a slope of 0.002, the intake was horizontal, and its elevation was level with the sediment bed of the main channel. The intake channel was located 9 meters downstream of the upstream stilling basin and 3 meters upstream of the water level control gate at the end of the flume. The water circulation system of the flume was with water supplied from interconnected underground reservoirs beneath the flume. The inlet flow rate was controlled using adjustable valves at the pump station. The flow depth was regulated using gates located at the ends of both the main

2026, Instituto Mexicano de Tecnología del Agua.
Open Access bajo la licencia CC BY-NC-SA 4.0
(https://creativecommons.org/licenses/by-nc-sa/4.0/)

and intake channels. To measure flow in the main and intake channels, rectangular and triangular sharp-crested weirs were used, and water depth was measured using a point gauge.

After the dimensional analysis, the experimental program was designed. To assess the behavior and determine the impact of the independent parameters on the sediment diverted to the intake, experiments were conducted. Due to space, laboratory, and time constraints, the range of changes for the parameters were selected accordingly. The first group of experiments was conducted without skimming wall structure. The second to fifth experimental groups investigated the effects of key geometric parameters of skimming walls on sediment control at the intake. These included wall spacing (10, 20, 30 cm), wall length (60, 75, 90 cm), wall height (2, 4, 6 cm), and the angle of the second branch relative to the main flow direction (1, 15, 30°). Each test was conducted under four flow rates (30, 40, 50, and 60 $\frac{\text{Lit}}{\text{Sec}}$). After each run, the volume of sediment entering the intake (V) was recorded. Further details are provided in supplemental data 2.

In all experimental groups, the effects of distance, length, height, angle, and flow variations on controlling sediment input to the intake were studied experimentally. As shown in Figure 3, the distance between the two walls, their angle relative to the main flume flow direction, as well as their length and height, are illustrated. The flow skimming walls are constructed of Plexiglas. The flow is steady and subcritical, with a fixed intake angle of 60°. The sediment particle diameter was kept constant at 1 mm, and the flow was classified as clear water.

2026, Instituto Mexicano de Tecnología del Agua.
Open Access bajo la licencia CC BY-NC-SA 4.0
(https://creativecommons.org/licenses/by-nc-sa/4.0/)

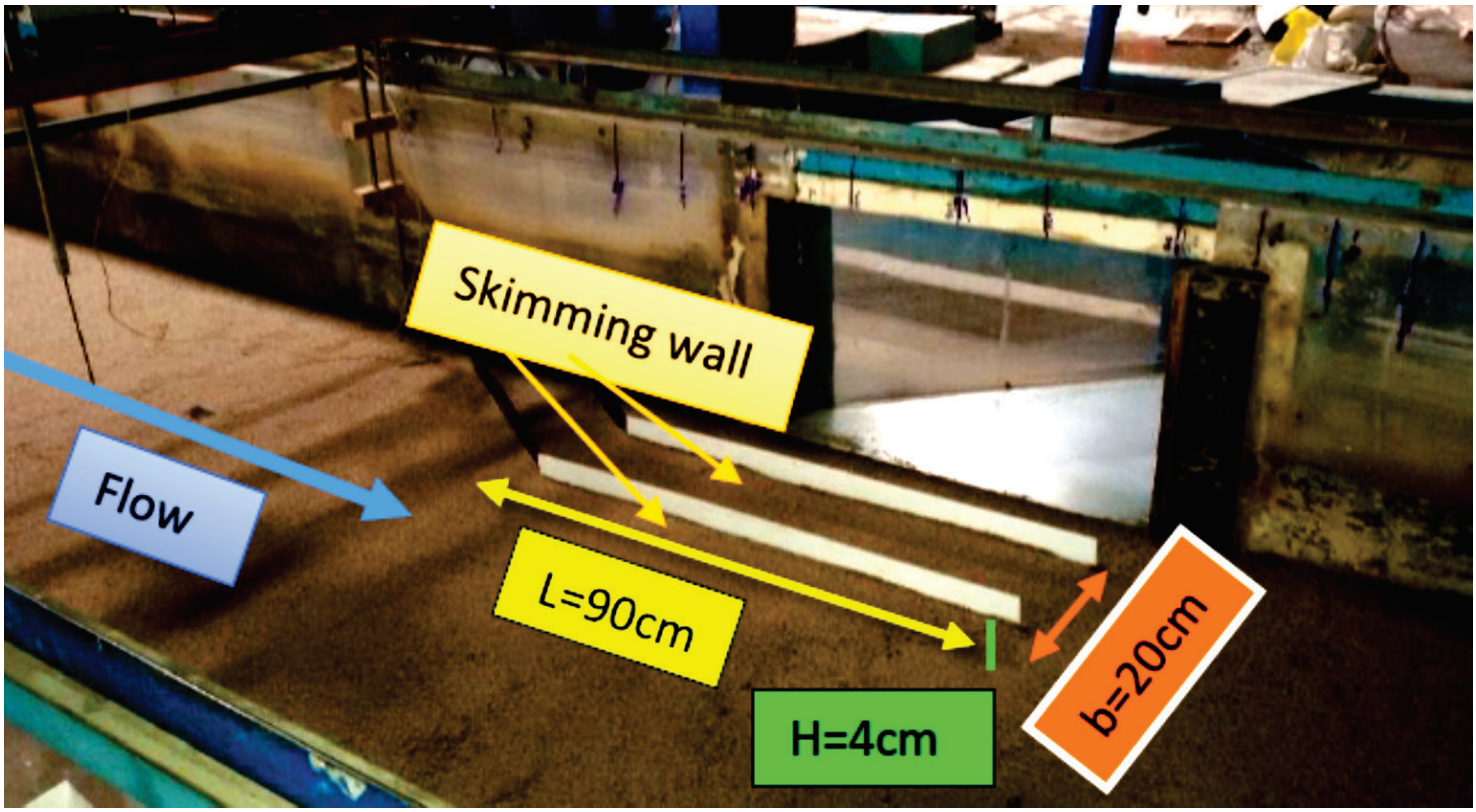


Figure 3. The position of the parallel skimming walls in the channel.

The main flume, measuring 12 m in length, 1.5 m in width, and 0.9 m in height, is equipped with a recirculating flow system. A 60 cm wide, 2.5 m long intake channel branches off at a 60° angle, located 9 m downstream of the stilling basin and 3 m upstream of the control gate. A 12 m³ reservoir supplies the flow, and water depth is regulated by gates at the downstream ends of both channels. An overview of the flume setup is shown in Figure 4.

2026, Instituto Mexicano de Tecnología del Agua.
Open Access bajo la licencia CC BY-NC-SA 4.0
(https://creativecommons.org/licenses/by-nc-sa/4.0/)



Figure 4. A view of the main channel interior and the measuring equipment.

Figure 5 shows the side and interior view of the rectangular channel in the absence of the control structure, and the intake structure is made of metal with transparent walls constructed from Plexiglas. The flume is equipped with a water level control gate at its downstream end and a sediment trap basin, while Figure 6 illustrates the rectangular weir installed upstream of the channel, a rectangular weir was used at the end of the main and secondary channels to measure the flow rate. Additionally, the flow depth was measured using both fixed and movable depth gauges with an accuracy of 0.1 mm.

2026, Instituto Mexicano de Tecnología del Agua.
Open Access bajo la licencia CC BY-NC-SA 4.0
(https://creativecommons.org/licenses/by-nc-sa/4.0/)

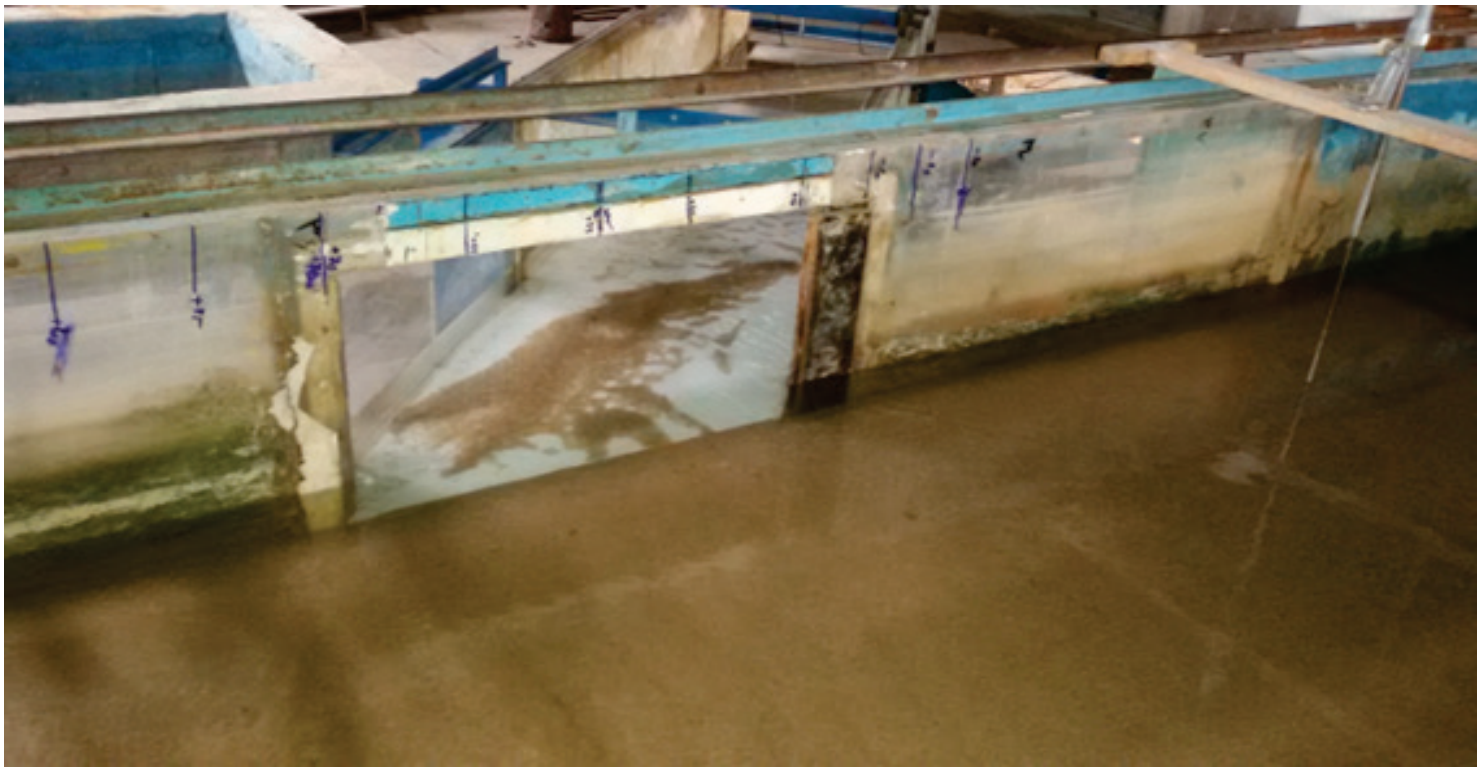


Figure 5. A view of the interior of the intake channel in the absence of the sediment control structure.

2026, Instituto Mexicano de Tecnología del Agua. Open Access bajo la licencia CC BY-NC-SA 4.0 (https://creativecommons.org/licenses/by-nc-sa/4.0/)



Figure 6. The rectangular weir used in the experimental process.

Selecting sediment material that realistically simulates natural bed load is a key challenge in experimental studies. To ensure bed load transport without suspension, sand with a 1 mm average diameter, specific gravity of 2.65 $\frac{\text{gr}}{\text{cm}^3}$ standard deviation of 1.47, and uniformity coefficient of 2.2 was used. Experimental conditions included a 25 l/s discharge, 0.002 bed slope, 4.6 cm flow depth, 0.0452 m hydraulic radius, and 0.03 m/s shear velocity. These conditions ensured that the selected sediment moved as bed load. Figure 7 presents the grain size distribution, with standard deviation and uniformity coefficient calculated using equations (5) and (6).

2026, Instituto Mexicano de Tecnología del Agua.
Open Access bajo la licencia CC BY-NC-SA 4.0
(https://creativecommons.org/licenses/by-nc-sa/4.0/)

$$\sigma_g = \left(\frac{D_{84}}{D_{16}}\right)^{0.5} = \left(\frac{1.22}{0.56}\right)^{0.5} = 1.47 \quad (5)$$

$$C_u = \frac{D_{60}}{D_{10}} = \frac{1.1}{0.6} = 2.20 \quad (6)$$

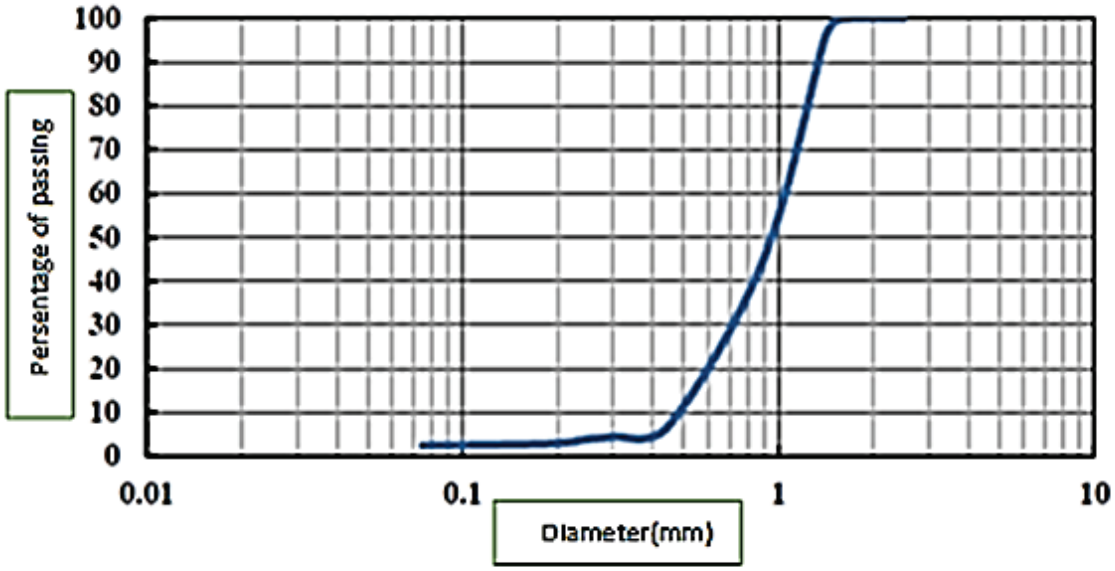


Figure 7. The grain size distribution curve of the bed sediments.

In the present study, the equations were derived using nonlinear regression of the experimental data. To validate these equations, statistical indices must be used to ascertain how closely the equations match the experimental data. In all the equations obtained in this study, the coefficient of determination (R^2) and the root mean square error (RMSE) are used as indices for validation, which statistically measure the proximity of the data to the fitted regression line. The mathematical expression of the RMSE index is as follows:

2026, Instituto Mexicano de Tecnología del Agua.
Open Access bajo la licencia CC BY-NC-SA 4.0
(https://creativecommons.org/licenses/by-nc-sa/4.0/)

$$\mathrm{RMSE} = \sqrt{\frac{1}{n}\sum_{i=1}^{n}(C_{s(Cal.)} - C_{s(Obs.)})^2} \quad (7)$$

In this study, sediment control equations were developed using laboratory data and dimensional analysis based on Buckingham's Pi Theorem. To simplify the influence of various factors on sediment transport into intakes, dimensionless parameters were used. A curve-fitting method was applied to derive a general equation relating the sediment control index (Π) to key dimensionless variables. Here, $C_{s(Cal.)}$ and $C_{s(Obs.)}$ denote the calculated and observed values, respectively, and the error index ideally close to zero—measures their difference.

$$C_s = \frac{V}{D^3} = A[Q_R]^{\alpha}[F_r]^{\mu}\left[\frac{b}{H}\right]^{\lambda}\left[\frac{L}{b}\right]^{\omega}[\theta]^{\phi} \quad (8)$$

Where:

$A, \mu, \lambda, \omega, \phi$ = constant values that will be obtained through the fitting of experimental data.

Results and discussion

General equation of C_{s1} for different channel widths (b)

In this section, the pattern and degree of influence of the dimensionless numbers are examined in a combined form $C_{s1} = \frac{V}{D^3}$. For a fixed skimming wall height (H = 4 cm) and a constant length (L=90cm), the equation

2026, Instituto Mexicano de Tecnología del Agua.
Open Access bajo la licencia CC BY-NC-SA 4.0
(https://creativecommons.org/licenses/by-nc-sa/4.0/)

between these numbers for different b values is expressed in a combined manner. In this case, the equation C_{s1} is derived using experimental data and curve-fitting tools, as shown Equation (9):

$$C_{S1} = \frac{V}{D^3} = 1.44[Q_R]^{-0.45}[F_r]^{2.16}\left[\frac{b}{H}\right]^{-0.005}\left[\frac{L}{b}\right]^{0.61} \quad (9)$$

Table 1 presents the parameters used, and the validation of Equation (9) with experimental data is shown in Figure 8. For 12 experiments conducted in three groups of four, with variations in channel width b (distance between walls), an appropriate RMSE and R2 of model was derived. The sensitivity percentage of Equation (9) to changes in dimensionless variables has been presented (For more details see supplemental data 3).

2026, Instituto Mexicano de Tecnología del Agua.
Open Access bajo la licencia CC BY-NC-SA 4.0
(https://creativecommons.org/licenses/by-nc-sa/4.0/)

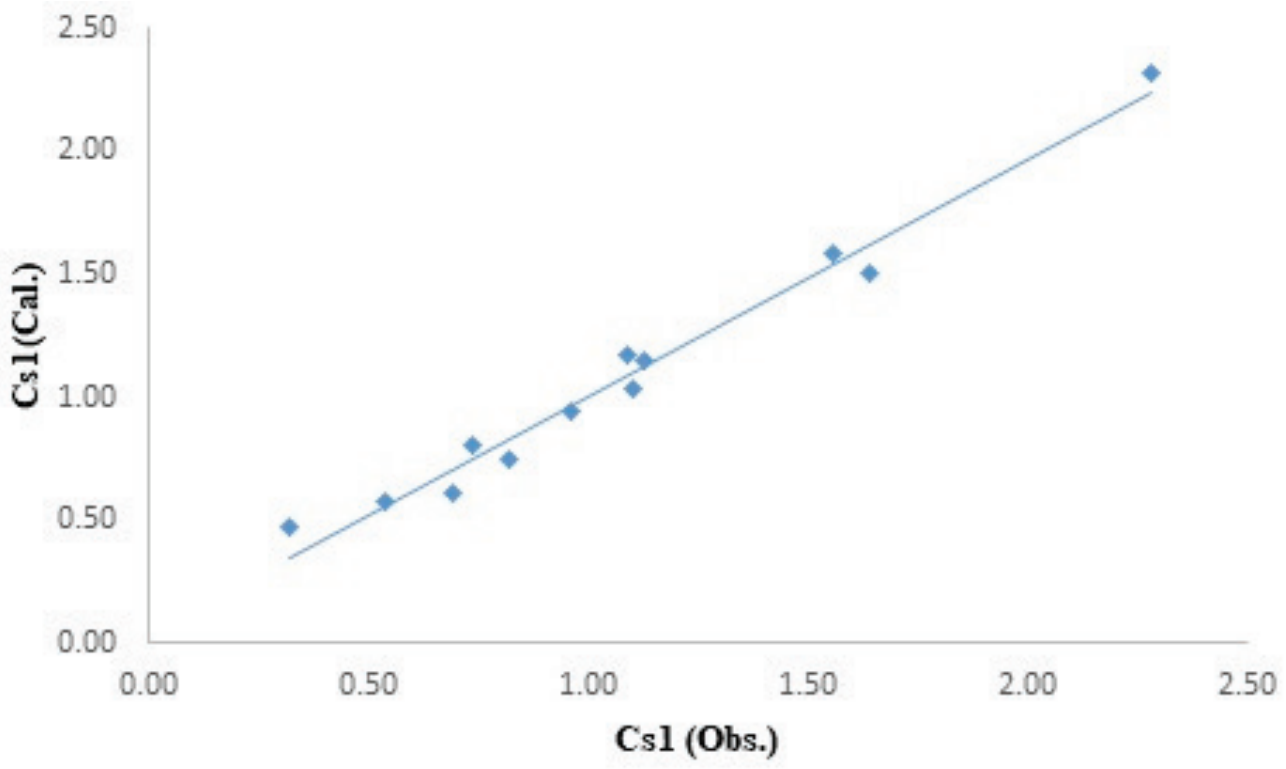


Figure 8. Validation of Equation (9) with experimental data.

The sensitivity analysis of Equation (9), regarding the removal of individual and combined dimensionless parameters, is presented in Table 2.

2026, Instituto Mexicano de Tecnología del Agua.
Open Access bajo la licencia CC BY-NC-SA 4.0
(https://creativecommons.org/licenses/by-nc-sa/4.0/)

Table 2. The sensitivity analysis of the model regarding the removal of dimensionless parameters for Equation (9).

Rows	A	α	μ	λ	ω	R^2	RMSE
1	1.44	-0.45	2.16	-0.005	0.61	0.98	0.0779
2	1.47	0	1.56	-0.004	0.62	0.97	0.0869
3	1.45	1.12	0	-0.005	0.61	0.91	0.1545
4	1.42	-0.45	2.16	0	0.62	0.98	0.0779
5	9.87	-0.45	2.16	-0.62	0	0.98	0.0779
6	7.36	0	0	-0.96	-0.32	0.39	0.4034
7	4.07	-0.38	2.10	0	0	0.55	0.3449
8	4.13	1.15	0	0	0	0.50	0.3664
9	4.14	0	1.58	0	0	0.55	0.3464
10	1.45	0	1.56	0	0.62	0.97	0.0869
11	10.05	0	1.56	-0.62	0	0.97	0.0869
12	1.43	1.12	0	0	0.62	0.91	0.1545
13	9.87	1.12	0	-0.62	0	0.91	0.1545
14	0.37	0	0	0	0.63	0.39	0.4034
15	2.69	0	0	-0.63	0	0.39	0.4034

General equation of C_{S2} for different values of (L)

In this section, the pattern and degree of influence of $C_{s2} = \frac{V}{D^3}$ from dimensionless numbers are examined in a combined manner. For a fixed skimming wall height (H = 4 cm) and a fixed distance between the walls (b = 20 cm), for different values of (L), the relationship with the dimensionless numbers is expressed in a combined form. This relationship

2026, Instituto Mexicano de Tecnología del Agua.
Open Access bajo la licencia CC BY-NC-SA 4.0
(https://creativecommons.org/licenses/by-nc-sa/4.0/)

is derived using experimental data and curve fitting tools, as shown below equation.

$$C_{S2} = \frac{V}{D^3} = 22.87[Q_R]^{-0.48}[F_r]^{2.17}\left[\frac{L}{b}\right]^{-1.16} \quad (10)$$

The parameters used are presented in Table 3, and the validation of Equation (10) with the experimental data is shown in Figure 9. For 12 experiments conducted in three groups of four, with variations in the length (L) of the flow skimming walls, an appropriate RMSE and R2 of model was derived (More details are available in supplemental data 4).

Table 3. The data used in Equation (10).

Rows	L(m)	Q_R	F_r	$\frac{L}{b}$	$C_{S2}(Obs.)$	$C_{S2}(Cal.)$
1	0.9	0.16	0.30	4.5	0.69	0.71
2	0.9	0.28	0.37	4.5	0.82	0.85
3	0.9	0.35	0.45	4.5	1.10	1.17
4	0.9	0.43	0.56	4.5	1.64	1.70
5	0.6	0.16	0.30	3	1.10	1.13
6	0.6	0.28	0.37	3	1.40	1.36
7	0.6	0.35	0.45	3	1.80	1.87
8	0.6	0.43	0.56	3	2.70	2.72
9	0.75	0.16	0.30	3.75	0.92	0.87
10	0.75	0.28	0.37	3.75	1.10	1.05
11	0.75	0.35	0.45	3.75	1.50	1.44
12	0.75	0.43	0.56	3.75	2.20	2.10

2026, Instituto Mexicano de Tecnología del Agua.
Open Access bajo la licencia CC BY-NC-SA 4.0
(https://creativecommons.org/licenses/by-nc-sa/4.0/)

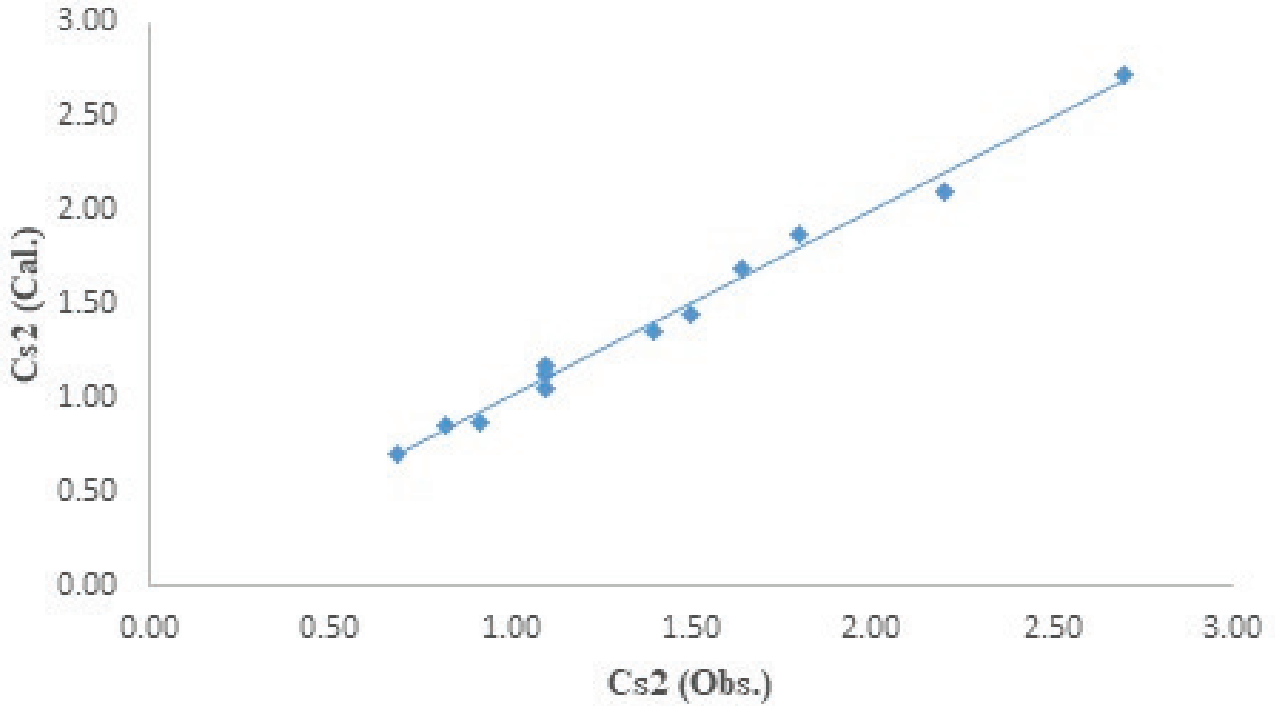


Figure 9. The validation of Equation (10) with experimental data.

The sensitivity analysis of Equation (10) regarding the removal of dimensionless parameters, both individually and in combination, is presented in Table 4.

2026, Instituto Mexicano de Tecnología del Agua.
Open Access bajo la licencia CC BY-NC-SA 4.0
(https://creativecommons.org/licenses/by-nc-sa/4.0/)

Table 4. Sensitivity analysis of the model regarding the removal of dimensionless parameters for Equation (10).

Rows	A	α	μ	ω	R^2	RMSE
1	22.87	-0.48	2.17	-1.16	0.99	0.0539
2	5.08	-0.49	2.19	0	0.73	0.2979
3	5.02	1.08	0	0	0.64	0.3438
4	5.18	0	1.52	0	0.72	0.3028
5	23.32	0	1.52	-1.16	0.98	0.0762
6	22.73	1.08	0	-1.17	0.90	0.1816
7	6.36	0	0	-1.16	0.24	0.4979

General equation of C_{S3} for different values of (H)

In this section, the pattern and extent of the impact of $\mathbf{C_{S3}} = \frac{\mathbf{V}}{\mathbf{D^3}}$ from dimensionless numbers are examined collectively. For a fixed length of the skimming walls (L = 90 cm) and a fixed distance between the walls (b = 20 cm), in various (H) values, the relationship between them and the dimensionless numbers is expressed combinatorically. The equation in this case is obtained using experimental data and curve fitting tools as follows:

$$C_{S3} = \frac{V}{D^3} = 2.44[Q_R]^{-0.61}[F_r]^{2.36}\left[\frac{b}{H}\right]^{0.26} \quad (11)$$

The parameters used are presented in Table 5, and the validation of Equation (11) with the experimental data is shown in Figure 10. For 12 experiments conducted in three groups of four, with variations in the high

2026, Instituto Mexicano de Tecnología del Agua.
Open Access bajo la licencia CC BY-NC-SA 4.0
(https://creativecommons.org/licenses/by-nc-sa/4.0/)

(H) of the flow skimming walls, an appropriate RMSE and R^2 of model was derived (More details are available in supplemental data 5).

Table 5. The data used in Equation (11) are provided.

Rows	H(m)	Q_R	F_r	$\frac{b}{H}$	$C_{S3}(Obs.)$	$C_{S3}(Cal.)$
1	0.04	0.16	0.30	5	0.69	0.67
2	0.04	0.28	0.37	5	0.82	0.78
3	0.04	0.35	0.45	5	1.10	1.08
4	0.04	0.43	0.56	5	1.64	1.59
5	0.06	0.16	0.30	3.33	0.65	0.60
6	0.06	0.28	0.37	3.33	0.70	0.70
7	0.06	0.35	0.45	3.33	0.90	0.97
8	0.06	0.43	0.56	3.33	1.40	1.43
9	0.02	0.16	0.30	10	0.75	0.80
10	0.02	0.28	0.37	10	0.94	0.94
11	0.02	0.35	0.45	10	1.29	1.30
12	0.02	0.43	0.56	10	1.91	1.91

2026, Instituto Mexicano de Tecnología del Agua.
Open Access bajo la licencia CC BY-NC-SA 4.0
(https://creativecommons.org/licenses/by-nc-sa/4.0/)

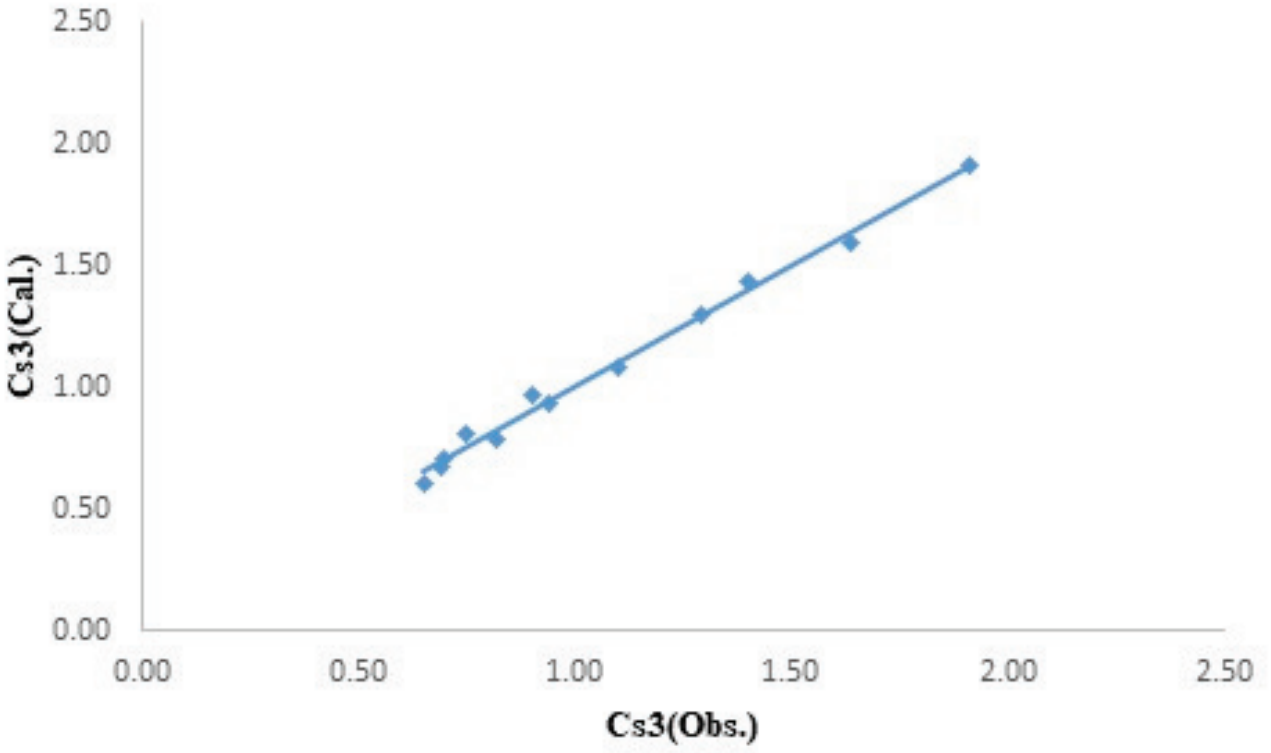


Figure 10. The validation of Equation (11) with experimental data is shown.

The sensitivity analysis of Equation (11) regarding the removal of dimensionless parameters, both individually and collectively, is presented in Table 6.

2026, Instituto Mexicano de Tecnología del Agua.
Open Access bajo la licencia CC BY-NC-SA 4.0
(https://creativecommons.org/licenses/by-nc-sa/4.0/)

Table 6. Sensitivity analysis of the model concerning the removal of dimensionless parameters for Equation (11).

Rows	A	α	μ	λ	R^2	RMSE
1	2.44	-0.61	2.36	0.26	0.99	0.0362
2	3.82	-0.64	2.38	0	0.87	0.1419
3	3.77	1.07	0	0	0.75	0.2001
4	3.91	0	1.53	0	0.85	0.1514
5	2.49	0	1.53	0.26	0.97	0.0625
6	2.40	1.08	0	0.27	0.87	0.1449
7	0.69	0	0	0.25	0.10	0.3730

General equation for C_{S4} in different θ Conditions

In this section, the pattern and sensitivity of $C_{S4} = \frac{V}{D^3}$ to dimensionless numbers are examined in a combined manner. For a fixed length of the separating walls (L = 90 cm), a fixed distance between the walls (b = 20 cm), and the height of the walls above the bed (H = 4 cm) under different θ conditions, the relationship with dimensionless numbers is expressed in a combined form. The equation for C_{S4} in this case is derived using the experimental data and curve fitting tools as follows:

$$C_{S4} = \frac{V}{D^3} = 3.76[Q_R]^{-0.72}[F_r]^{2.46}[\theta]^{0.25} \quad (12)$$

The parameters used in this study are presented in Table 7, and the validation of Equation (12) with the experimental data is depicted by Figure 11. For 12 experiments conducted in three groups of four, with

2026, Instituto Mexicano de Tecnología del Agua.
Open Access bajo la licencia CC BY-NC-SA 4.0
(https://creativecommons.org/licenses/by-nc-sa/4.0/)

variations in the angle between the flow skimming walls and the main flow direction of the flume. (θ) of the flow skimming walls, an appropriate RMSE and R^2 of model was derived (More details are available in supplemental data 6).

Table 7. The data used in Equation (12).

Rows	Q_R	F_r	θ (Degree)	$C_{S4}(Obs.)$	$C_{S4}(Cal.)$
1	0.16	0.30	1	0.69	0.72
2	0.28	0.37	1	0.82	0.81
3	0.35	0.45	1	1.10	1.12
4	0.43	0.56	1	1.64	1.65
5	0.16	0.30	15	1.38	1.41
6	0.28	0.37	15	1.64	1.58
7	0.35	0.45	15	2.20	2.18
8	0.43	0.56	15	3.28	3.22
9	0.16	0.30	30	1.70	1.67
10	0.28	0.37	30	1.88	1.87
11	0.35	0.45	30	2.50	2.58
12	0.43	0.56	30	3.80	3.82

2026, Instituto Mexicano de Tecnología del Agua.
Open Access bajo la licencia CC BY-NC-SA 4.0
(https://creativecommons.org/licenses/by-nc-sa/4.0/)

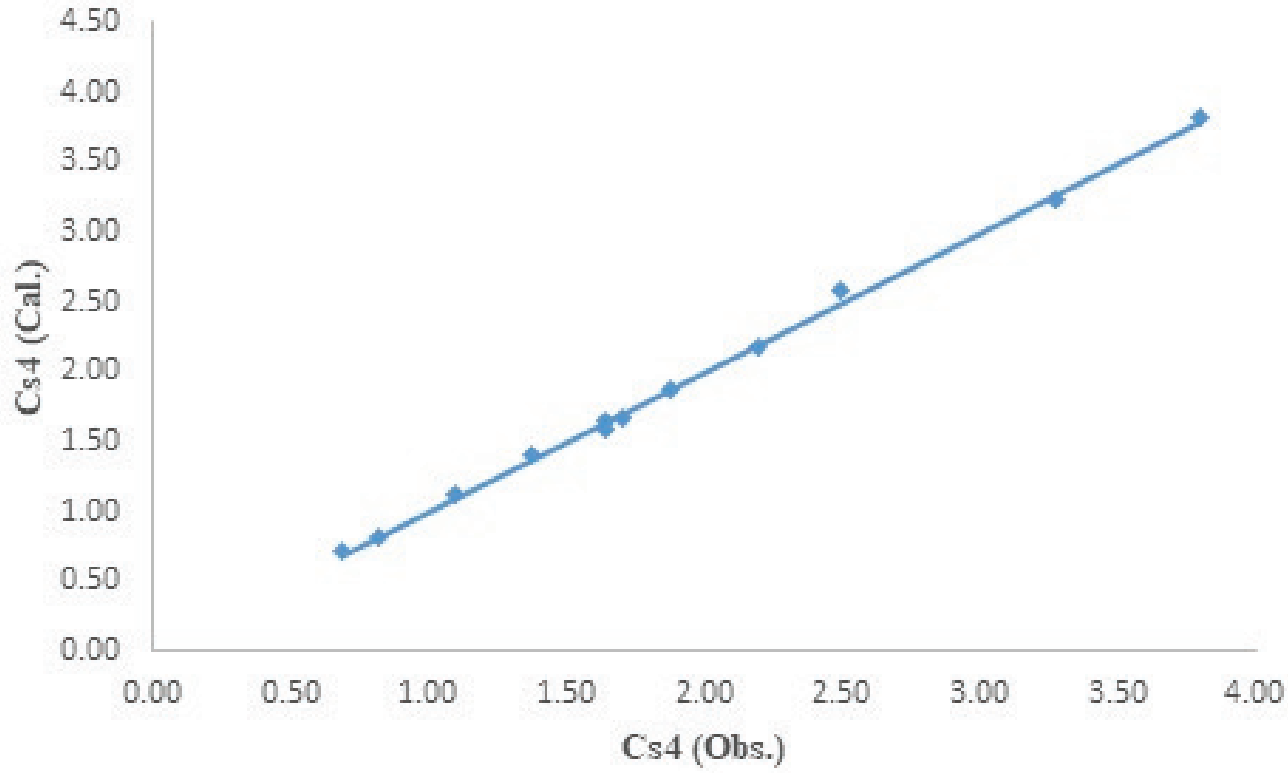


Figure 11. Validation of Equation (12) with experimental data.

The sensitivity analysis of Equation (12), regarding the removal of dimensionless parameters both individually and combined, is presented in Table 8.

Table 8. A summary of the model's sensitivity analysis with respect to the removal of dimensionless parameters for Equation (12) is provided.

Rows	A	α	μ	∅	R^2	RMSE
1	3.76	-0.72	2.46	0.25	0.99	0.0393
2	3.86	0	1.50	0.24	0.98	0.1180
3	1.07	0	0	0.25	0.44	0.6695
4	1.07	0	1.50	0	0.49	0.6396

2026, Instituto Mexicano de Tecnología del Agua.
Open Access bajo la licencia CC BY-NC-SA 4.0
(https://creativecommons.org/licenses/by-nc-sa/4.0/)

Charts 8, 9, 10, and 11 show the trends of changes in $\mathbf{C_{s1}}$, $\mathbf{C_{s2}}$, $\mathbf{C_{s3}}$, and $\mathbf{C_{s4}}$, respectively, in both computational and observational states, which ultimately led to the development of unique equations for each of the $\mathbf{C_s}$ parameters. In Tables 2, 4, 6 and 8, the results related to the root mean square and the variance associated with equations (9), (10), (11), and (12), considering the experimental data, are presented. As can be observed, the derived equations are of a linear type and the unique equations, and the variances indicate this, with the obtained equations being the results of these validations. The observed trends in sediment reduction using parallel skimming walls are consistent with the fundamental mechanisms reported in previous studies on lateral intake sediment control. Similar to the findings of Barkdoll *et al*. (1999), increasing the spacing between guiding structures (b/H) significantly reduces the transverse momentum of near-bed flow entering the intake, resulting in a substantial decrease in sediment entrainment. The present results further quantify this effect, showing that b/H = 7.5 yields up to an 86 % reduction in sediment entry, which is in close agreement with the performance ranges reported by Moradinejad *et al*. (2017) for optimized intake geometries. The strong influence of the Froude number, as reflected by the high exponents (2.16–2.46) in Equations (9)-(12), confirms that sediment entry is primarily governed by flow inertia and turbulence intensity. This observation aligns with classical sediment transport theories and experimental findings that associate higher Froude numbers with increased suspension and transverse sediment transport toward the intake. Conversely, geometric parameters with small exponents (e.g., b/H in Eq. 9 or θ in Eq. 12) play a secondary but stabilizing role by controlling flow alignment and suppressing vortex formation near the intake entrance. Compared to conventional sediment-

2026, Instituto Mexicano de Tecnología del Agua.
Open Access bajo la licencia CC BY-NC-SA 4.0
(https://creativecommons.org/licenses/by-nc-sa/4.0/)

control devices such as submerged vanes or sills, the parallel skimming wall configuration examined in this study offers comparable or superior sediment reduction efficiency while maintaining structural simplicity and reduced construction complexity. This advantage makes the proposed configuration particularly suitable for practical applications in irrigation and water diversion systems.

These results extend previous studies by providing quantitative predictive equations and sensitivity-based design guidance. Overall, the results demonstrate a consistent and physically meaningful response of sediment entry to both hydraulic and geometric parameters across all experimental configurations. The derived equations not only capture the observed trends with high accuracy but also clarify the relative importance of flow inertia, discharge ratio, and wall geometry in controlling sediment transport toward the intake. By combining validation results with sensitivity analyses, the present study provides a clearer interpretation of how parallel skimming walls modify near-bed flow structure and reduce sediment entrainment under different operating conditions. To address the details of experimental uncertainty, factors such as standard deviation, potential measurement tool errors, curve-fitting methods, and the influence of different parameters on model accuracy should be considered. When comparing with experimental data, variations in parameters like channel width, wall height, and angle (θ) can significantly impact the results. Since these parameters often have specific ranges of variation, the models presented in the paper should be sensitive to these changes. Sensitivity analysis in this regard helps to precisely identify the impact of each parameter on the final model, ultimately improving the accuracy and predictive capabilities of the

2026, Instituto Mexicano de Tecnología del Agua.
Open Access bajo la licencia CC BY-NC-SA 4.0
(https://creativecommons.org/licenses/by-nc-sa/4.0/)

models. Therefore, to write a paragraph about the details of experimental uncertainty, the following points can be highlighted:

1. Measurement uncertainty: Potential inaccuracies associated with the measurement instruments (e.g., for channel dimensions and flow properties) have been acknowledged, and their impact on recorded values is considered.
2. Curve fitting methods: The use of curve-fitting tools and the estimation of fixed parameters (such as A, μ, λ, and ...) may introduce estimation errors. We now discuss how these uncertainties affect the model calibration process.
3. A detailed sensitivity analysis is included to assess how variations in geometric and physical parameters (such as channel width, wall height, and inclination angle θ) influence the model outcomes. This helps quantify the robustness of the model. This analysis highlights which parameters have the strongest effect on model accuracy, helping to interpret the robustness of the predictions
4. Modeling errors: We also acknowledge the inherent modeling errors due to simplifications and assumptions made during the model development process, especially when extrapolating from experimental data.

Conclusion

This experimental study demonstrated that parallel skimming walls can effectively reduce sediment entry into lateral intakes while offering a simpler alternative to conventional sediment-control structures. The results showed that sediment inflow is strongly influenced by hydraulic

2026, Instituto Mexicano de Tecnología del Agua.
Open Access bajo la licencia CC BY-NC-SA 4.0
(https://creativecommons.org/licenses/by-nc-sa/4.0/)

conditions, particularly the intake discharge ratio (Q_R) and the Froude number (F_r), which consistently exhibited the highest sensitivity in all derived models. Among the investigated geometric parameters, the spacing between walls (b/H) had the greatest impact on sediment reduction, with b/H = 7.5 achieving up to an 86 % decrease in sediment entry. Increasing the wall length (L/b) further enhanced performance, while maintaining a near-parallel alignment ($\theta \approx 1°$) proved more effective than inclined configurations. These findings provide clear design guidelines for optimizing sediment control at side intakes. Sensitivity analyses confirmed that removing F_r or Q_R from the predictive equations significantly reduced model accuracy, highlighting their dominant role in sediment transport mechanisms. The derived equations offer reliable predictive tools within the tested parameter ranges and can support preliminary design and optimization of lateral intakes. Future studies should extend the present work by considering unsteady flow conditions, different sediment gradations, and field-scale validations to further enhance the applicability of the proposed configurations.

Funding

The authors declare that no funding support was received for the preparation of this article.

Statement on conflicts of interest

The authors declare no conflict of interest.

2026, Instituto Mexicano de Tecnología del Agua. Open Access bajo la licencia CC BY-NC-SA 4.0 (https://creativecommons.org/licenses/by-nc-sa/4.0/)

Statement on the use of AI

The authors declare that no Artificial Intelligence tools were used in the preparation of this article.

Data availability statement

The raw data supporting the conclusions of this article will be made available by the authors upon request.

Supplementary materials

Notation

Symbol	Unit	Description
Q_R	$\frac{m^3}{S}$	Discharge (Flow Rate)
b	m	Width of Channel
U,V,W	$\frac{m}{s}$	Velocity of Components
X, Y, Z	-	Direction of Flow in Channel
C	-	Sediment Concentration
D	-	Diffusion Coefficient of Sediment
S	-	sediment source/sink term
g	$\frac{m}{s^2}$	Gravitational Acceleration
L	m	Length of the Skimming Walls
H	m	Flow Depth
σ_g	-	Standard Deviation

2026, Instituto Mexicano de Tecnología del Agua.
Open Access bajo la licencia CC BY-NC-SA 4.0
(https://creativecommons.org/licenses/by-nc-sa/4.0/)

Symbol	Unit	Description
G_s	$\frac{g}{cm^3}$	Specific Mass
ρ_s	$\frac{g}{cm^3}$	Sediment Density
C_u	-	Uniform Coefficient
F_r	-	Froude Number
θ	Degree	Angle of Skimming Walls to the Horizon
τ_b	$\frac{N}{m^2}$	Bed Shear Stress

Supplemental data

Supplemental data 1. Parameters affecting the sediment flow entering the side intake.

Parameters	Abbreviation	Parameter Type in the Current Study
Flow Rate in the main Channel	$\mathbf{Q_m}$	Variable
Flow rate in the Intake Channel	$\mathbf{Q_L}$	Variable
Flow Depth in the main Channel	$\mathbf{D}$	Variable
Flow Velocity in the main Channel	$\mathbf{V_m}$	Variable
Flow Velocity in the Intake Channel	$\mathbf{V_L}$	Variable
Width of the main Channel	$\mathbf{B_m}$	Constant
Width of the Intake Channel	$\mathbf{B_L}$	Constant
Slope of the main Channel	$\mathbf{S_m}$	Constant
Slope of the Intake Channel	$\mathbf{S_L}$	Constant
Gravitational Acceleration	$\mathbf{g}$	Constant
Flow Density	$\boldsymbol{\rho}$	Constant

2026, Instituto Mexicano de Tecnología del Agua. Open Access bajo la licencia CC BY-NC-SA 4.0 (https://creativecommons.org/licenses/by-nc-sa/4.0/)

Parameters	Abbreviation	Parameter Type in the Current Study
Kinematic Viscosity of Fluid	ν	Constant
Angle between the Intake Channel and the main Channel	γ	Constant
Angle between Skimming Wall Structure and the Shore	β	Constant
Height of Skimming Wall Plates	H	Variable
Length of the Initial Branches of the Skimming Wall	L_0	Constant
Length of the Second Branches of the Skimming Wall	L	Variable
Experiment Time	t	Constant
Average Diameter of Bed Sediments	d_{50}	Constant
Density of Sediments	ρ_s	Constant
Bed Roughness	K_s	Constant
Distance between Skimming Walls	b	Variable
Angle of the Second Branch of the Skimming Walls with the main Flow Direction	θ	Variable
Volume of Sediment Entering the Intake	V	Variable

Supplemental data 2. Values of variables in the experiments.

Parameters	$Q_m\left(\frac{lit}{sec}\right)$	$Q_L\left(\frac{lit}{sec}\right)$	$D(cm)$	F_r	Q_r
State 1	30	4.8	7.7	0.30	0.16
State 2	40	11.2	8.1	0.37	0.28
State 3	50	17.5	8.2	0.45	0.35
State 4	60	25.8	8.0	0.56	0.43

2026, Instituto Mexicano de Tecnología del Agua.
Open Access bajo la licencia CC BY-NC-SA 4.0
(https://creativecommons.org/licenses/by-nc-sa/4.0/)

Tecnología y Ciencias del Agua
OPEN ACCESS
Check for updates

Supplemental data 3. Statistical Information for the Validation of Equation (9) with experimental data.

Type of equation	Equation	R^2	RMSE
Leaner	$C_{s1(Cal.)} = 0.96C_{s1(Obs.)} + 0.041$	0.98	0.0779

Supplemental data 4. The validation of Equation (10) with experimental data.

Type of equation	Equation	R^2	RMSE
Leaner	$C_{s2(Cal.)} = 0.99C_{s2(Obs.)} + 0.014$	0.99	0.0539

Supplemental data 5. Statistical validation data of Equation (11) with experimental results.

Type of equation	Equation	R^2	RMSE
Leaner	$C_{s3(Cal.)} = 0.99C_{s3(Obs.)} + 0.003$	0.99	0.0362

Supplemental data 6. Statistical information for the validation of Equation (12) with experimental data.

Type of equation	Equation	R^2	RMSE
Leaner	$C_{s4(Cal.)} = 0.99C_{s4(Obs.)} + 0.0079$	0.99	0.0393

2026, Instituto Mexicano de Tecnología del Agua.
Open Access bajo la licencia CC BY-NC-SA 4.0
(https://creativecommons.org/licenses/by-nc-sa/4.0/)

References

Attarzadeh, A., & Ghodsian, M. (2018). رسوب کنترل میزان و جریان جدایی عرض مطالعه جانبی آبگیر در مختلف های سامانه در [Study on flow separation width and control over the sediments in various systems of lateral intake]. In: *17th National Hydraulic Conference*, Shahr Kord, Iran. https://civilica.com/doc/811415/

Barkdoll, B. D., Ettema, R., & Odgaard, A. J. (1999). Sediment control at lateral diversions: Limits and enhancements to vane use. *Journal of Hydraulic Engineering*, *125*(8), 862-870. https://doi.org/10.1061/(ASCE)0733-9429(1999)125:8(862)

Bor, A. (2022). Experimental investigation of 90° intake flow patterns with and without submerged vanes under sediment feeding conditions. *Canadian Journal of Civil Engineering*, *49*(3), 452-463. https://doi.org/10.1139/cjce-2020-0616

Chen, J. C., Cheng, C. Y., Huang, C. L., & Chen, S. C. (2020). Assessment of the visual quality of sediment control structures in mountain streams. *Water*, *12*(11), 3116. https://doi.org/10.3390/w12113116

Davoodi, L., & Shafiei-Bijestan, M. (2012). آبگیر به ورودی رسوب بر جریان شرایط تاثیر مستغرق صفحات بدون و با حالت دو در جانبی [The effect of flow conditions on sediment entry to lateral intakes in two cases with and without submerged plates]. In: *4th Iranian Water Resources Management Conference*, Amirkabir University of Technology, Tehran, Iran. https://civilica.com/doc/117137/

2026, Instituto Mexicano de Tecnología del Agua.
Open Access bajo la licencia CC BY-NC-SA 4.0
(https://creativecommons.org/licenses/by-nc-sa/4.0/)

Golej, H., Haghabi, A., Sanei, M., & Yonesi, H. A. (2019). آزمایشگاهی بررسی در درجه 75 جانبی آبگیر به بستر ورودی رسوب کنترل در دیوارجداکننده و آبشکن ،آستانه کاربرد قوس U شکل [Experimental study of the application of sill, dike and skimming wall in controlling bed sediment entering 75° lateral intake in a U channel bend]. *Journal of Irrigation and Water Engineering*, *9*(3), 18-37. https://doi.org/10.22125/iwe.2019.88629

Habibi, H., Masjedi, A., Purmohammadi, M. H., Kamanbedast, A. A., & Bordbar, A. (2019). Experimental analysis of the effect of geometric shape of submerged vanes on sedimentation flows at lateral intake entrance in river bends. *Irrigation Sciences and Engineering*, *42*(2), 119-133. https://doi.org/10.22055/jise.2017.22614.1614

Halvaeifard, M., & Masjedi, A. (2017). رسوب کنترل در مستغرق صفحات زاویه اثر بررسی رودخانه درجه ۱۸۰ قوس در جانبی آبگیر به [Study of the effect of the angle of submerged vanes on sediment control in lateral intake at a 180 degree river arc]. *JWSS-Isfahan University of Technology*, *20*(78), 29-38. https://doi.org/10.18869/acadpub.jstnar.20.78.29

Hsu, C. C., Tang, C. J., Lee, W. J., & Shieh, M. Y. (2002). Subcritical 90° equal-width open-channel dividing flow. *Journal of Hydraulic Engineering*, *128*(7), 716-720. https://doi.org/10.1061/(ASCE)0733-9429(2002)128:7(716)

Johnson, P. A., Hey, R. D., Tessier, M., & Rosgen, D. L. (2001). Use of vanes for control of scour at vertical wall abutments. *Journal of Hydraulic Engineering*, *127*(9), 772-778. https://doi.org/10.1061/(ASCE)0733-9429(2001)127:9(772)

2026, Instituto Mexicano de Tecnología del Agua.
Open Access bajo la licencia CC BY-NC-SA 4.0
(https://creativecommons.org/licenses/by-nc-sa/4.0/)

Kuriqi, A., Koçileri, G., & Ardiçlioğlu, M. (2020). Potential of Meyer-Peter and Müller approach for estimation of bed-load sediment transport under different hydraulic regimes. *Modeling Earth Systems and Environment*, *6*(1), 129-137. https://doi.org/10.1007/s40808-019-00665-0

Mandal, A., Gautam, H., & Ahmad, Z. (2024). Sediment control and flow redistribution with submerged vanes: a review. *Water Practice & Technology*, *19*(5), 2197-2212. https://doi.org/10.2166/wpt.2024.131

Moradinejad, A., Haghiabi, A. H., Saneie, M., & Yonesi, H. (2016). Experimental study of the effect of spur dike location and skimming wall on divertion of flow and sediment at lateral intake. *Journal of Irrigation and Drainage Engineering*, *17*(67), 145-162. https://doi.org/10.22092/aridse.2017.109611

Moradinejad, A., Haghiabi, A. H., Saneie, M., & Yonesi, H. (2017). Investigating the effect of a skimming wall on controlling the sediment entrance at lateral intakes. *Water Supply*, *17*(4), 1121-1132. https://doi.org/10.2166/ws.2017.007

Nakato, T., & Ogden, F. L. (1998). Sediment control at water intakes along sand-bed rivers. *Journal of Hydraulic Engineering*, *124*(6), 539. https://doi.org/10.1061/(ASCE)0733-9429(1998)124:6(589)

Sharma, H., & Ahmad, Z. (2020). Turbulence characteristics of flow past submerged vanes. *International Journal of Sediment Research*, *35*(1), 42-56. https://doi.org/10.1016/j.ijsrc.2019.07.002

2026, Instituto Mexicano de Tecnología del Agua.
Open Access bajo la licencia CC BY-NC-SA 4.0
(https://creativecommons.org/licenses/by-nc-sa/4.0/)

Tabrizi, H., Haghiabi, A., Saneie, M., & Younesi, H. (2017). سازه اثر بررسی آبراهه قوس در واقع جانبی آبگیرهای رسوب و جریان هیدرولیک بر آبشکن [Evaluation of spur dike effect on sediment and flow hydraulic of side intakes located on channel bends]. *Watershed Engineering and Management*, *9*(3), 346-359. https://jwem.areeo.ac.ir/article_112376.html?lang=en

Wibowo, M., Hendriyono, W., Rahman, R. A., Susatijo, G., Kongko, W., Istiyanto, D. C., Widagdo, A. B., Nugroho, S., Khoirunnisa, H., Wiguna, E., Aziz, H., & Santoso, B. (2020). Sediment transport modeling at Jelitik Estuary, Sungailiat-Bangka Regency for the design of sediment control structures. *Journal of Physics: Conference Series*, *1625*, 012042. https://doi.org/10.1088/1742-6596/1625/1/012042

2026, Instituto Mexicano de Tecnología del Agua.
Open Access bajo la licencia CC BY-NC-SA 4.0
(https://creativecommons.org/licenses/by-nc-sa/4.0/)